

Original Article

Chimeric MrNV-GE11-VLPs serve as a nano-container to deliver Doxorubicin into cancer cells

Khwanthana Grataitong^{1,2}, Charoonroj Chotwiwatthanakun^{3,4}, Orawan Thongsum¹, Krittalak Chakrabandhu⁵, and Wattana Weerachatanukul^{1*}

¹ Department of Anatomy, Faculty of Science, Mahidol University, Ratchathewi, Bangkok, 10400 Thailand

² Department of Basic Medical Science, Faculty of Medicine Vajira Hospital, Navamindradhiraj University, Dusit, Bangkok, 10300 Thailand

³ Center of Excellence for Shrimp Molecular Biology and Biotechnology, Faculty of Science, Mahidol University, Ratchathewi, Bangkok, 10400 Thailand

⁴ Mahidol University, Nakhonsawan campus, Payuha Khiri, Nakhon Sawan, 60130 Thailand

⁵ Equipe labellisée La Ligue, Institute of Signaling, Developmental Biology and Cancer Research, CNRS-UMR, Nice, 6543 France

Received: 27 January 2022; Revised: 27 October 2022; Accepted: 18 November 2022

Abstract

We have reported that virus-like particle from shrimp virus, MrNV-VLP, effectively encapsulates and delivers plasmid DNA and dsRNA into Sf9 insect cells and shrimp tissues. Additionally, modifying VLP with GE-11 peptide extension on the surface (so called, E-MrNV-GE11-VLP) allows them to interact specifically with the EGFR-positive SW480 cancer cells. This work extrapolated the use of E-MrNV-GE11-VLP to encapsulate and deliver doxorubicin (DOX) towards SW480 cells. The results showed that DOX was passively loaded into VLPs in a molar ratio of >200 DOX/VLP equivalent to a loading efficiency of 3%. Specific targeting of E-MrNV-GE11-VLP + DOX and its anti-cancer effect towards SW480 was more pronounced than that of N-MrNV-VLP + DOX, suggesting an interaction and internalization of E-MrNV-GE11-VLP through surface EGFR. This claim was also supported by a lower DOX delivery into MCF7 than SW480 cells. Finally, the cell cytotoxicity assay showed that E-MrNV-GE11-VLP + DOX significantly decreased cell viability in SW480 cells more than that by N-MrNV-VLP + DOX ($P < 0.05$), while its cytotoxicity effect on MFC7 cells was much lower than on SW480 cells. This study provides insights into how to develop target-specific drug delivery for carrying therapeutic agents towards specific tumor cells.

Keywords: MrNV, VLP, colorectal cancer, EGFR, doxorubicin

1. Introduction

Macrobrachium rosenbergii nodavirus (MrNV) is a shrimp infectious, non-enveloped virus with an icosahedral

symmetry (T=3) and a size of 26-27 nm in diameter (Bonami, Shi, Qian, & Sri Widada, 2005; Owens, La Fauce, Juntunen, Hayakijkosol, & Zeng, 2009; Sahul Hameed, Yoganandhan, Sri Widada, & Bonami, 2004; Yoganandhan, Leartvibhas, Sriwongpuk, & Limsuwan, 2006; Zhang *et al.*, 2014). The self-assembling VLP was generated from their capsid protein which is encoded by the RNA2 gene (Bonami *et al.*, 2005;

*Corresponding author

Email address: wattana.wee@mahidol.ac.th

Goh, Tan, Bhassu, & Tan, 2011). Apart from its simplicity, also its superior physical properties, as well as its controllable particle assembly, are outstanding superior to the other reported VLPs. MrNV-VLP is tolerant of many harsh conditions, especially resistant against strong digestive enzyme digestion (Jariyapong *et al.*, 2014). The controllability of MrNV-VLPs to encapsulate nucleotide-based agents (DNA vector and dsRNA) through the uses of EGTA and DTT (specific calcium chelator and reducing agent, respectively) is also well established (Jariyapong *et al.*, 2014, 2015). Notably, most of the placement sites of the foreign epitopes onto the exterior surface of VLPs are modulated through any individual loop of the protruding (P) domain at the C-terminus leading to a binding enhancement of the VLPs (Ho *et al.*, 2018). Chimeric MrNV-VLP was modified for their C-terminus by M2e (matrix 2 protein, a foreign epitope of influenza A) to induce a type-1 T-helper immune response (Yong, Yeap, Ho, Omar, & Tan, 2015). Moreover, inserting HBsAg (hepatitis B surface antigen) onto the MrNV-VLP's surface significantly increases the levels of natural killer and cytotoxic T-cells as well as enhances interferon-gamma (IFN- γ) secretion (Yong, Yeap, Goh, *et al.*, 2015). Recently, we have constructed chimeric MrNV-VLP with GE11 peptide (known to specifically target epithelial growth factor receptor, EGFR) by conjugating the peptide into the C-terminal end of MrNV capsid protein (E-MrNV-GE11-VLP) to improve its binding and internalization into the EGFR-positive cancer cells, SW480 (Grataitong *et al.*, 2021). This strategic nanocontainer design and the superior physical properties of MrNV-VLP mentioned above have opened up the opportunity to develop a promising nanocontainer as a drug delivery tool to fight against EGFR-positive cancers.

Doxorubicin (DOX) is a chemotherapeutic compound that is commonly used in the treatment of various types of cancers. The anti-tumor effect of DOX has been known to block topoisomerase-II resulting in DNA damage (Kim, Lee, & Kim, 2009) and generating reactive oxygen species (ROS) leading to cell cycle arrest, oxidative stress, and cancer cell death (Tsang, Chau, Kong, Fung, & Kwok, 2003). However, limitations of DOX applications are from low water solubility and strong side effects including congestive heart failure and toxicity to normal cells (Renu, V, P, & Arunachalam, 2018). To overcome these serious complications, a specific nanocontainer that has the ability to encapsulate this compound and specifically deliver it through a ligand-receptor modulation towards the cancer cells should be developed. In fact, recent reports have demonstrated that encapsulation of DOX into VLP's cavity may utilize 3 main approaches including 1) passive encapsulation through interior modification with hydrophobic peptide (NS5A₁₋₃₁) (Buehler *et al.*, 2014; Shan *et al.*, 2018), 2) infusion depending on pH and metal ion concentration (Prasuhn, Yeh, Obenaus, Manchester, & Finn, 2007; Wen *et al.*, 2012; Yildiz, Lee, Chen, Shukla, & Steinmetz, 2013), and 3) conjugation of DOX via EDC/NHS reaction to the capsid interior (Aljabali, Shukla, Lomonosoff, Steinmetz, & Evans, 2013; Yan *et al.*, 2017; Zhao *et al.*, 2011). An alternative approach has also been made to conjugate lysine residues of MrNV capsid with folic acid (FA) for delivering DOX to folic receptor overexpressing cancer cells (Thong, Biabanikhankahdani, Ho, Alitheen, & Tan, 2019). In this study, we aimed at testing the encapsulation efficiency of the chimeric E-MrNV-GE11-VLP to passively

encapsulate a hydrophobic cancer therapeutic agent, DOX, as well as to test the cell-specific delivery of chimeric VLP towards EGFR-positive cancer cells.

2. Materials and Methods

2.1. Expression and purification of chimeric MrNV-GE11-VLP

N-MrNV and E-MrNV-GE11 capsid sequences were synthesized and ligated into the pET16b expression vector by General Biosystems (Morrisville, NC). Transformation of the recombinant vector into competent *Escherichia coli* (BL21) was performed by the heat shock method (42°C, 45 sec) and immediately followed by ice incubation (5 min). Transformed *E. coli* were inoculated in SOC (Super Optimal Broth) medium (Invitrogen, Grand Island, NY) until the absorbance of 0.6–0.8 at 600 nm (A₆₀₀) was reached. Protein expression was induced by adding 1 mM IPTG to the culture followed by an overnight incubation (16 h, 25°C). After harvesting, the cells were ruptured by sonication (100 Hz, 20 sec, 10 cycles) and centrifuged (12,000×g, 10 min). The supernatant was loaded onto a Nickel column chromatography. After several washes with a washing buffer (PBS, 500 mM NaCl, 20 mM imidazole, pH 7.4), bound proteins were eluted with elution buffer (PBS, 500 mM NaCl, 250 mM imidazole, pH 7.4). The proteins were dialyzed against PBS overnight at 4 °C and further subjected to filtration through a Centricon device (cut-off 50 kDa) centrifuged at 5,000 ×g (15 min, 4°C). The upper retentate was collected and the concentrations of purified N-MrNV-VLP and E-MrNV-GE11_VLP were measured by NanoDrop2000 Spectrophotometer (Thermo Fisher Scientific, Delaware).

2.2. Encapsulation of DOX into MrNV-VLPs

N-MrNV-VLPs and E-MrNV-GE11-VLPs were incubated with 2.5 M urea at 25 °C for 3 h to disassemble the VLP particles (Shen *et al.*, 2015). Different concentrations of DOX were prepared in DMSO and mixed with 2 mg of the dissociated VLPs (2 h) with gentle agitation in dark at 25 °C. The mixtures were dialyzed in an assembling buffer (50 mM Tris-HCl, 100 mM NaCl, pH 8.6, 10 % glycerol) at 4 °C for 48 h to reassemble VLPs. The chimeric VLPs were filtered through a Centricon centrifugal device at 5,000×g (cut-off 50 kDa, 15 min, 4°C) and the protein concentration was analyzed using a UV-VIS Detector at 280 nm (for protein) and 495 nm (for DOX). BCA assay was also performed to determine the protein concentrations of both VLPs. The entrapment efficiency (EE), loading efficiency (LE), and the molar ratio of DOX (M_{DOX}) for each VLP were calculated by using the following equations described previously (Hong *et al.*, 2013; Zeng *et al.*, 2013):

$$EE\% = \text{Weight}_{\text{DOX loaded}} / \text{Weight}_{\text{total DOX loaded}} \times 100\%$$

$$LE\% = \text{Weight}_{\text{DOX loaded}} / \text{Weight}_{\text{MrNV-VLPs}} \times 100\%$$

$$M_{\text{DOX}} = LE \times (MW_{\text{MrNV-VLP}} / MW_{\text{doxorubicin}})$$

2.3 Confocal fluorescence microscopy

In vitro localization of the chimeric MrNV-GE11-VLPs with or without DOX were assessed by confocal

fluorescence microscopy. Aldehyde-fixed cells were treated with 30 mM glycine in PBS and washed twice with PBS containing 0.2% Tween 20 (PBST). Non-specific antibody staining was blocked with 4% BSA prior to incubation with mouse anti-MrNV antibody (1:500) followed by Alexa488 - conjugated goat anti-mouse antibody at a dilution of 1:1,000 (Invitrogen, Eugene, CA). Cells were counterstained with 4', 6-diamidino-2-phenylindole dihydrochloride (DAPI) for nuclear visualization. For confocal microscopy, the images were acquired by an Olympus FV1000 confocal microscope using argon and krypton laser lines and the emission filters of 460 nm and 520 nm band-pass types. A line-by-line with Kalman's scanning mode was also applied to minimize a cross interaction of emission beams.

2.4 Cell cytotoxicity

Cytotoxicity of N-MrNV-VLP and E-MrNV-GE11-VLP with or without DOX was assessed by MTT assay following the method described previously (Al-Ziaydi, Al-Shammari, Hamzah, Kadhim, & Jabir, 2020). SW480 cells (EGFR-positive) and MCF7 (EGFR-negative) cells were seeded in 96-well plates with 5×10^3 cells/well and cultured overnight. The growth medium was removed and then replaced with 200 μ L of fresh medium containing 0-20 μ g/mL N-MrNV-VLP, E-MrNV-GE11-VLP, N-MrNV-VLP + DOX, E-MrNV-GE11-VLP + DOX, and free DOX for 24 h, respectively. After rinsing with PBS, the cells were treated for another 4 h in 0.5 mg/mL MTT solution (Invitrogen, Carlsbad, CA). Finally, the solution was removed and 100 μ L DMSO was added to each well. The absorbance of each sample was measured at 490 nm by a MK3 Reader (ThermoFisher Scientific, Hillsboro, OR). The obtained data were statistically analyzed using an unpaired *t*-test with GraphPad Prism (Jabir, 2019).

3. Results

3.1 Production of both MrNV-VLPs and their loading of DOX into VLPs

Both MrNV-VLPs were produced in *E. coli* and purified by a Nickel affinity chromatography. Both purified MrNV capsid proteins were collected in the eluted fractions and their profiles showed single-banded proteins at the molecular masses of 42.5 kDa (for N-MrNV-VLP) and 43.5 kDa (for E-MrNV-GE11-VLP) with the purity of >95% (Grataitong *et al.*, 2021). Loading of DOX into N-MrNV-VLPs and E-MrNV-GE11-VLPs was performed using a urea-based encapsulation method mentioned in Materials and Methods and is depicted for ease of understanding in Figure 1A. When subjected to fluorospectrometric analysis, two peaks of fluorescent absorbance at 280 nm and 495 nm were observed for both N-MrNV-VLP + DOX and E-MrNV-GE11-VLP + DOX (Figure 1B), indicating the successful loading of DOX into the VLP's cavity. The entrapment efficiencies (EE) of the N-MrNV-VLP + DOX and E-MrNV-GE11-VLP + DOX were $5.54 \pm 0.4\%$ and $7.18 \pm 0.48\%$, respectively, while the loading efficiencies (LE) were $2.75 \pm 0.1\%$ and $3.702 \pm 0.1\%$, respectively. The molar ratios (M_{DOX}) were 211.0 ± 10.0 and 298.9 ± 9.8 of DOX loaded into N-MrNV-VLP and E-MrNV-GE11-VLP, respectively.

3.2 Confocal microscopy of DOX delivery into SW480 and MCF 7 cells

Deliveries of the free DOX, N-MrNV-VLP + DOX, and E-MrNV-GE11-VLP + DOX were analyzed in the two cancer cell lines, SW480 colorectal cancer cell line (overexpressing EGFR) and MCF7 cell line (expressing very low level of EGFR). As positive controls, SW480 and MCF7 cells treated with the free DOX revealed an intense, red fluorescence signal in the nuclei (Figures 2 and 3, row 2), a known localization of DOX staining upon its uptake into the cells (Biabanikhankahdani, Alitheen, Ho, & Tan, 2016). Comparatively, SW480 cells incubated with N-MrNV-VLP + DOX showed a much lower fluorescent intensity compared to those incubated with E-MrNV-GE11-VLP + DOX which showed a relatively high fluorescent intensity in the nuclei (Figures 2, rows 3 and 4) resembling that of free DOX treatment. This result demonstrated that modification of VLP with GE11 peptide enhanced SW480 cellular uptake of DOX loaded into VLP's cavity. Supporting this claim was the higher internalization of E-MrNV-GE11-VLP-DOX into SW480 cells than of N-MrNV-VLP + DOX (Figure 2, column 4).

MCF7 cells incubated with N-MrNV-VLP + DOX and E-MrNV-GE11-VLP + DOX exhibited a lower intensity of red fluorescence in the nuclei than MCF7 cells incubated with free DOX (Figure 3, compare rows 3 and 4 with row 2). The results in Figures 2 and 3 clearly demonstrated the non-specific cellular uptake of free DOX into the cells, no matter whether they are expressing EGFR on the cell surfaces. In addition, the absence of anti-MrNV staining in any groups of MCF7 cell treatments (Figure 3, column 4) also supported our

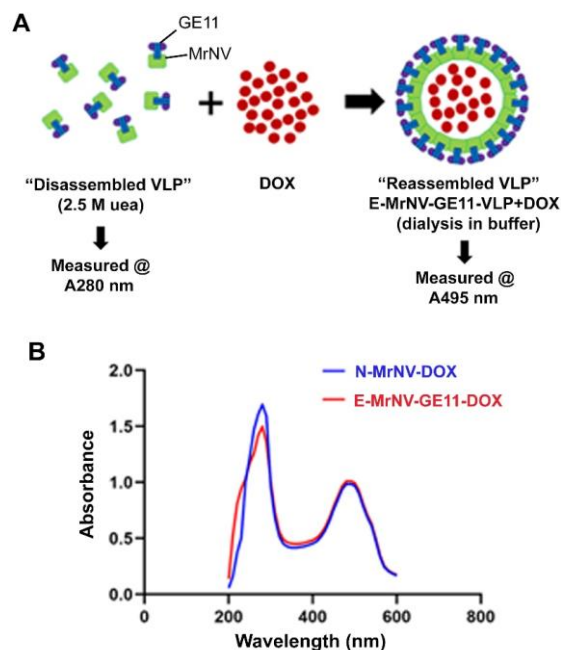


Figure 1. Schematic diagram depicting the encapsulation method through disassembly and reassembly of VLP for preparing E-MrNV-GE11-VLP + DOX and its fluorospectrometric detection (A). The absorbance profiles of N-MrNV-VLP + DOX (blue line) and E-MrNV-GE11-VLP + DOX (red line) at 280 nm and 495 nm are shown in B.

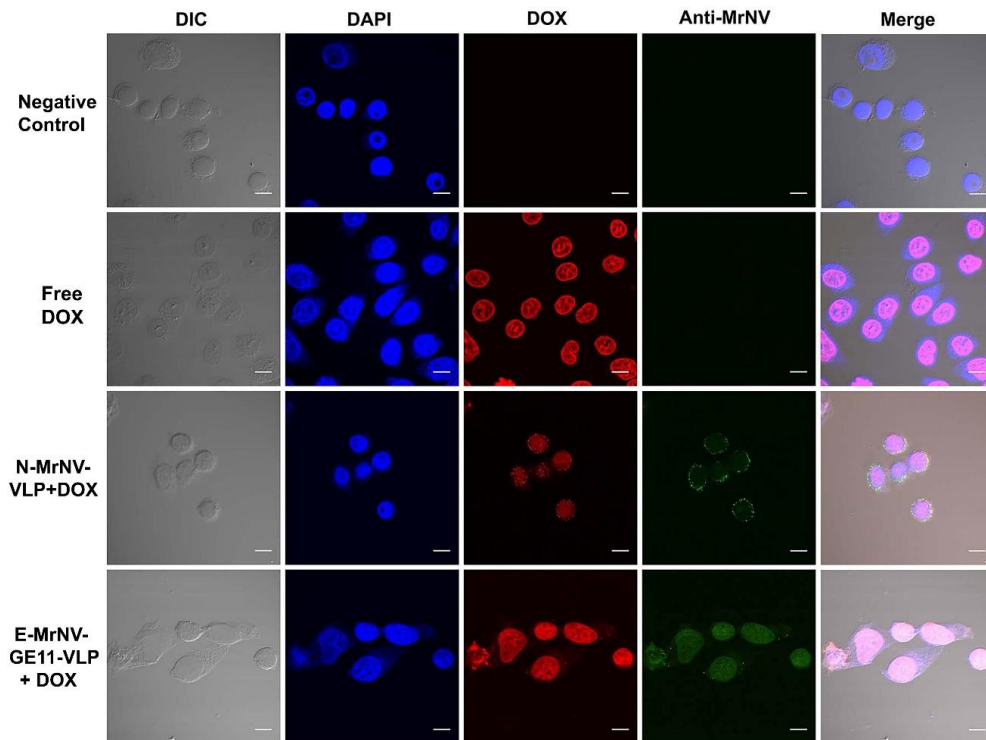


Figure 2. Confocal microscopy of *in vitro* delivery of DOX by the chimeric E-MrNV-GE11-VLP + DOX into SW480 cells at T=120 min. SW480 cells were incubated with empty VLP (row 1), free DOX (row2), N-MrNV-VLP + DOX (Row3) and E-MrNV-GE11-VLP + DOX (Row4). The staining of monoclonal anti-MrNV antibody and Alexa-488 conjugated secondary antibody is shown in green, whereas the staining of DOX and DAPI are shown in red and blue, respectively. Bars = 50 μm.

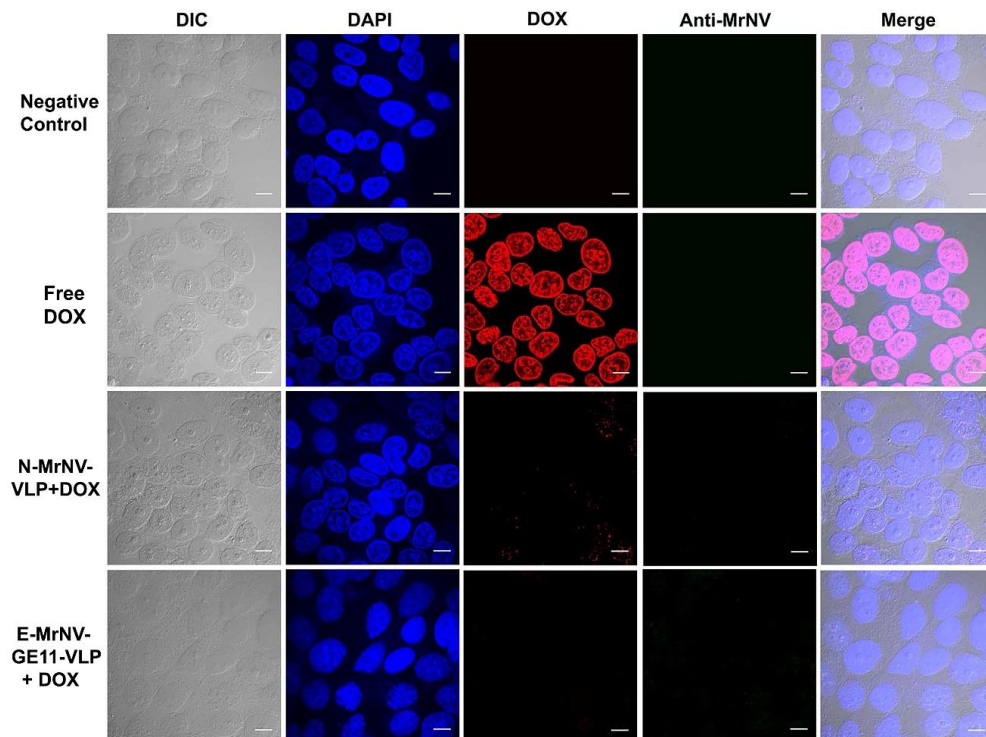


Figure 3. Confocal microscopy of *in vitro* delivery of DOX by the chimeric E-MrNV-GE11-VLPs + DOX into MCF7 cells at T=120 min. All treatment conditions were similar to those mentioned for SW480 cells above (in Figure 2) and the staining panels are anti-MrNV antibody + Alexa-488 conjugated secondary antibody (green), DOX (red) and DAPI (blue). Bars = 50 μm.

claim that delivery of E-MrNV-GE11-VLP + DOX was by receptor-mediated internalization into EGFR positive SW480 cells, but not into MCF7 cells. Negative controls where the cells were incubated with empty MrNV VLP or PBS did not show any red fluorescent signal in the nuclei (Figures 2 and 3).

3.3 Cytotoxicity of MrNV-GE11-VLPs-DOX on SW480 and MCF7 cells

We used the MTT assay to monitor the cytotoxicity of various regimens for DOX treatments including free DOX, N-MrNV-VLP + DOX, and E-MrNV-GE11-VLP + DOX at the concentrations of 0-20 $\mu\text{g/ml}$ towards SW480 and MCF7 cells. As a strong cancer therapeutic agent, free DOX treated SW480 cells showed the percent viability reduced to $70.72 \pm 1.53\%$ even with only 1 $\mu\text{g/ml}$ of free DOX. However, at this same concentration, the percent cell viability in the groups of N-MrNV-VLP + DOX and E-MrNV-GE11-VLP + DOX was markedly reduced to $45.76 \pm 0.78\%$ and $31.20 \pm 2.54\%$, respectively, which was considered a statistically significant difference ($P < 0.01$) (Figure 4A, **). For E-MrNV-GE11-VLP + DOX treatment, a gradual decrease in the cell viability was observed towards 20 $\mu\text{g/ml}$, at which dose only $13.3 \pm 0.77\%$ cell viability remained. By calculation, the IC_{50} values of the 3 testing regimens on SW480 cells were $0.9634 \mu\text{g/ml}$, $0.4481 \mu\text{g/ml}$ and $0.2258 \mu\text{g/ml}$.

Treatments of MCF7 with these regimens greatly differed from those of SW480, namely 87-90% cell viability was still seen at 1 $\mu\text{g/ml}$ in all treatment groups and the cell viability was reduced much slower in all three groups even at the concentration of 20 $\mu\text{g/ml}$ (except for the free DOX which gave the relatively low percent viability of $46 \pm 7.67\%$) (Figure 4B). The calculated IC_{50} values for MCF7 cells were $9.550 \mu\text{g/ml}$, $7.149 \mu\text{g/ml}$ and $11.92 \mu\text{g/ml}$, respectively. Together, the results demonstrated that E-MrNV-GE11-VLP + DOX greatly reduced cell viability in SW480 cells, which was presumably due to specific targeting (and thus internalization) of E-MrNV-GE11-VLP + DOX towards EGFR receptors, which were numerously present on the surface of SW480 cells. As a consequence, a local accumulation of DOX within their cytoplasm could be expected. Negative controls where empty chimeric VLPs or PBS, which when used to treat the cells showed no cytotoxicity on either the SW480 or the

MCF7 cells (data not shown).

4. Discussion

Conventional chemotherapy is the major treatment for cancer patients; however, a limitation of this treatment is the encountered severe side effects due to the non-specific distribution of therapeutic agents into normal tissues (Renu *et al.*, 2018). Doxorubicin (DOX) is commonly used in the treatment of various cancers, but its limitations in clinical use include low solubility in buffer and enormous non-desirable effects (Kim *et al.*, 2009; Tsang *et al.*, 2003), which require considerable attention in the care. As an anthracycline chemical, DOX has two main anti-tumor mechanisms. First, it intercalates DNA molecules and blocks topoisomerase-II resulting in DNA damage (Kim *et al.*, 2009). Second, it generates an accumulation of reactive oxygen species (ROS) leading to cell cycle arrest, oxidative stress, and cancer cell death (Tsang *et al.*, 2003). However, DOX can attack not only cancer cells but also damages normal cells resulting in the severe side effects: both congestive heart failure and other cellular toxicity (Renu *et al.*, 2018). Thus, encapsulating it into chimeric VLP appears to be a promising solution to minimize these side effects, through the shielding of DOX cytotoxicity by the strong capsid shell (Chen, Zhang, Zhu, Xie, & Chen, 2017). In addition, its specific delivery to the targeted cancer tissue is highly advantageous for avoiding damage to the non-cancerous tissues. A recent excellent example is a conjugation of GE11 epitope (known to bind specifically to EGFR) to create chimeric VLP, which serves as a nano glue for enhancing its capacity to deliver therapeutic DOX into colorectal cancer cells (Grataitong *et al.*, 2021).

Due to its small size of about 545 Da and its hydrophobicity, DOX is shown to be one of the difficult compounds to encapsulate into VLPs. Thus, understanding DOX properties that lead to its packaging process into VLP is one of the steps that move us closer to the target-specific delivery of DOX, which enhances its cancer therapeutic efficiency while avoiding its severe side effects in the tissues. Recent reports have demonstrated that loading DOX into VLPs can be established through three main approaches including 1) passive encapsulation, 2) infusion, and 3) conjugation via EDC/NHS reactions. Our results showed that DOX could be packed into the E-MrNV-GE11-VLPs through a simple passive encapsulation. The compromised-passive

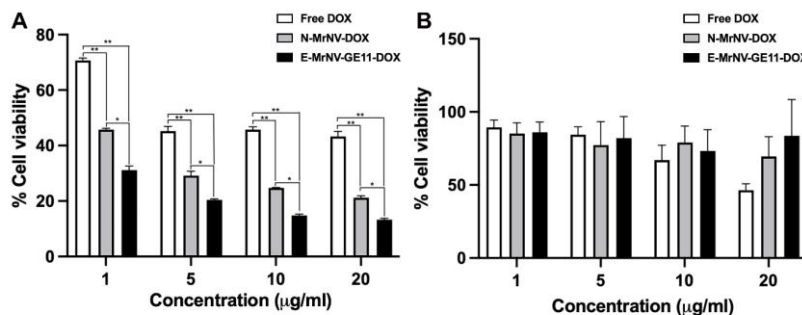


Figure 4. Cell viability post 24 h incubation with free-DOX, N-MrNV-VLP + DOX, and E-MrNV-GE11-VLP + DOX. Cultured SW480 (A) and MCF7 (B) cells were incubated with free and VLP-DOX at the concentrations of 0-20 $\mu\text{g/ml}$ and further subjected to MTT assay. Data are presented as mean \pm S.D. of triplicate experiments. Asterisks (*, **) indicate significant difference at $P < 0.05$ and $P < 0.01$, respectively.

encapsulation for MrNV-VLP (and other VLPs studied) might be explained by the inherent property of the *N*-terminus of MrNV capsid protein that engages both positively charged amino acid clusters (to interact with viral genome) and hydrophobic amino acid motifs in a randomized fashion (to interact with a hydrophobic-based compound such as DOX) (Jariyapong *et al.*, 2014). Although the molar ratio of DOX loading into VLP was about 200-300 DOX/VLP, still the loading efficiency into both types of MrNV-VLP was relatively low (about 3%) compared to the sizable cavity of 27-nm MrNV particle. Despite this low amount of encapsulation, DOX encapsulated VLPs still revealed a promising anti-cancer effect, in the treatment of SW480 cells with E-MrNV-GE11-VLP + DOX leading to a significant decrease in cell viability of this EGFR-positive cancer cell (Figure 4A). This can be explained by a specific affinity of the GE-11 peptide (that is decorated on the MrNV-VLP surface) with EGFR receptor (existing extensively on SW480 cell surface), leading to a local accumulation of DOX in their cytoplasm and thus lethal effect on the cells as mentioned above. This specificity of E-MrNV-GE11-VLP towards EGFR has also been confirmed by a much lower cytotoxicity effect of the E-MrNV-GE11 + DOX treatment in the MCF7 (Figure 4B), possibly due to the absence or low level of EGFR on its surface.

To improve DOX loading into the VLPs, HBc VLP engineering with hydrophobic peptide (NS5A₁₋₃₁) to their capsid interior significantly improves DOX delivery towards the tumor sites both *in vitro* and *in vivo* (Buehler *et al.*, 2014; Shan *et al.*, 2018). Alternatively, chemical conjugation of DOX via EDC/NHS reactions to the interior surface of many VLPs including CPMV, FMDV, and rotavirus structural protein VP6 VLPs could also enhance DOX loading efficiency (Aljabali *et al.*, 2013; Yan *et al.*, 2017; Zhao *et al.*, 2011). Lastly, altering electrostatic forces of the flexible, porous VLPs by adjusting pH and metal ion concentration could enhance the infused-small molecules locating into the capsid's cavity (Prasuhn *et al.*, 2007; Wen *et al.*, 2012; Yildiz *et al.*, 2013). In this regard, several VLPs including RCNMV, HBc, and HCRSV VLPs are able to pack DOX into their cavity by infusion of DOX with many small carriers such as RNA molecules (Lockney *et al.*, 2011; Thong *et al.*, 2019), polyacrylic acid (PAA) (Biabanikhankahdani *et al.*, 2016; Ren, Wong, & Lim, 2007) and polystyrene sulfonic acid (PSA) (Ren *et al.*, 2007). As for future perspective, we are now conducting the interior modification of this chimeric MrNV-GE11-VLP to enhance its encapsulation and targeting efficiency with the aim of using this nano-delivery system as a novel bioweapon in a new strategic target-specific cancer therapy.

Acknowledgements

This work was supported by the Royal Golden Jubilee Ph.D. Program, the Thailand Research Fund (TRF; Grant # PHD/0205/25517) and National Research Council of Thailand (NRCT; Grant # NRCT5-RSA 63015-02 to WW).

References

Al-Ziaydi, A. G., Al-Shammari, A. M., Hamzah, M. I., Kadhim, H. S., & Jabir, M. S. (2020). Newcastle

disease virus suppress glycolysis pathway and induce breast cancer cells death. *Virusdisease*, 31(3), 341-348. doi:10.1007/s13337-020-00612-z

- Aljabali, A. A., Shukla, S., Lomonossoff, G. P., Steinmetz, N. F., & Evans, D. J. (2013). CPMV-DOX delivers. *Molecular Pharmaceutics*, 10(1), 3-10. doi:10.1021/mp3002057
- Biabanikhankahdani, R., Alitheen, N. B. M., Ho, K. L., & Tan, W. S. (2016). pH-responsive Virus-like Nanoparticles with Enhanced Tumour-targeting Ligands for Cancer Drug Delivery. *Scientific Reports*, 6, 37891. doi:10.1038/srep37891
- Bonami, J. R., Shi, Z., Qian, D., & Sri Widada, J. (2005). White tail disease of the giant freshwater prawn, *Macrobrachium rosenbergii*: separation of the associated virions and characterization of MrNV as a new type of nodavirus. *Journal of Fish Diseases*, 28(1), 23-31. doi:10.1111/j.1365-2761.2004.00595.x
- Buehler, D. C., Marsden, M. D., Shen, S., Toso, D. B., Wu, X., Loo, J. A., . . . Rome, L. H. (2014). Bioengineered vaults: self-assembling protein shell-lipophilic core nanoparticles for drug delivery. *ACS Nano*, 8(8), 7723-7732. doi:10.1021/nn5002694
- Chen, H., Zhang, W., Zhu, G., Xie, J., & Chen, X. (2017). Rethinking cancer nanotheranostics. *Nature Review Materials*, 2. doi:10.1038/natrevmats.2017.24
- Goh, Z. H., Tan, S. G., Bhasu, S., & Tan, W. S. (2011). Virus-like particles of *Macrobrachium rosenbergii* nodavirus produced in bacteria. *Journal of Virological Methods*, 175(1), 74-79. doi:10.1016/j.jviromet.2011.04.021
- Grataitong, K., Huault, S., Chotwiwatthanakun, C., Jariyapong, P., Thongsum, O., Chawiwithaya, C., . . . Weerachatanukul, W. (2021). Chimeric virus-like particles (VLPs) designed from shrimp nodavirus (MrNV) capsid protein specifically target EGFR-positive human colorectal cancer cells. *Scientific Reports*, 11(1), 16579. doi:10.1038/s41598-021-95891-x
- Ho, K. L., Gabrielsen, M., Beh, P. L., Kueh, C. L., Thong, Q. X., Streetley, J., . . . Bhella, D. (2018). Structure of the *Macrobrachium rosenbergii* nodavirus: A new genus within the Nodaviridae? *Plos Biology*, 16(10), e3000038. doi:10.1371/journal.pbio.3000038
- Hong, W., Chen, D. W., Zhang, X. J., Zeng, J. F., Hu, H. Y., Zhao, X. L., & Qiao, M. X. (2013). Reversing multidrug resistance by intracellular delivery of Pluronic (R) P85 unimers. *Biomaterials*, 34(37), 9602-9614. doi:10.1016/j.biomaterials.2013.08.032
- Jabir, M. (2019). Evaluation of some immunological markers in children with bacterial meningitis caused by *Streptococcus pneumoniae*. *Research journal of biotechnology*, 14.
- Jariyapong, P., Chotwiwatthanakun, C., Direkbusarakom, S., Hirono, I., Wuthisuthimethavee, S., & Weerachatanukul, W. (2015). Delivery of double stranded RNA by *Macrobrachium rosenbergii* nodavirus-like particles to protect shrimp from white spot syndrome virus. *Aquaculture*, 435, 86-91. doi:https://doi.org/10.1016/j.aquaculture.2014.09.034

- Jariyapong, P., Chotwiwatthanakun, C., Somrit, M., Jitrapakdee, S., Xing, L., Cheng, H. R., & Weerachatanukul, W. (2014). Encapsulation and delivery of plasmid DNA by virus-like nanoparticles engineered from *Macrobrachium rosenbergii* nodavirus. *Virus Research*, 179, 140-146. doi:10.1016/j.virusres.2013.10.021
- Kim, H. S., Lee, Y. S., & Kim, D. K. (2009). Doxorubicin exerts cytotoxic effects through cell cycle arrest and Fas-mediated cell death. *Pharmacology*, 84(5), 300-309. doi:10.1159/000245937
- Lockney, D. M., Guenther, R. N., Loo, L., Overton, W., Antonelli, R., Clark, J., . . . Franzen, S. (2011). The Red clover necrotic mosaic virus capsid as a multifunctional cell targeting plant viral nanoparticle. *Bioconjugate Chemistry*, 22(1), 67-73. doi:10.1021/bc100361z
- Owens, L., La Fauce, K., Juntunen, K., Hayakijkosol, O., & Zeng, C. (2009). *Macrobrachium rosenbergii* nodavirus disease (white tail disease) in Australia. *Disease of Aquatic Organisms*, 85(3), 175-180. doi:10.3354/dao02086
- Prasuhn, D. E., Jr., Yeh, R. M., Obenaus, A., Manchester, M., & Finn, M. G. (2007). Viral MRI contrast agents: coordination of Gd by native virions and attachment of Gd complexes by azide-alkyne cycloaddition. *Chemical Communications*, (12), 1269-1271. doi:10.1039/b615084e
- Ren, Y., Wong, S. M., & Lim, L. Y. (2007). Folic acid-conjugated protein cages of a plant virus: a novel delivery platform for doxorubicin. *Bioconjugate Chemistry*, 18(3), 836-843. doi:10.1021/bc060361p
- Renu, K., V. G. A., P. B. T., & Arunachalam, S. (2018). Molecular mechanism of doxorubicin-induced cardiomyopathy - An update. *European Journal of Pharmacology*, 818, 241-253. doi:10.1016/j.ejphar.2017.10.043
- Sahul Hameed, A. S., Yoganandhan, K., Sri Widada, J., & Bonami, J. R. (2004). Experimental transmission and tissue tropism of *Macrobrachium rosenbergii* nodavirus (MrNV) and its associated extra small virus (XSV). *Disease of Aquatic Organisms*, 62(3), 191-196. doi:10.3354/dao062191
- Shan, W., Zhang, D., Wu, Y., Lv, X., Hu, B., Zhou, X., . . . Zhang, X. (2018). Modularized peptides modified HBc virus-like particles for encapsulation and tumor-targeted delivery of doxorubicin. *Nanomedicine: Nanotechnology, Biology, and Medicine*, 14(3), 725-734. doi:10.1016/j.nano.2017.12.002
- Shen, L., Zhou, J., Wang, Y., Kang, N., Ke, X., Bi, S., & Ren, L. (2015). Efficient encapsulation of Fe₃O₄ nanoparticles into genetically engineered hepatitis B core virus-like particles through a specific interaction for potential bioapplications. *Small*, 11(9-10), 1190-1196. doi:10.1002/sml.201401952
- Thong, Q. X., Biabanikhankahdani, R., Ho, K. L., Alitheen, N. B., & Tan, W. S. (2019). Thermally-responsive Virus-like Particle for Targeted Delivery of Cancer Drug. *Scientific Reports*, 9(1), 3945. doi:10.1038/s41598-019-40388-x
- Tsang, W. P., Chau, S. P., Kong, S. K., Fung, K. P., & Kwok, T. T. (2003). Reactive oxygen species mediate doxorubicin induced p53-independent apoptosis. *Life Sciences*, 73(16), 2047-2058. doi:10.1016/s0024-3205(03)00566-6
- Wen, A. M., Shukla, S., Saxena, P., Aljabali, A. A., Yildiz, I., Dey, S., . . . Steinmetz, N. F. (2012). Interior engineering of a viral nanoparticle and its tumor homing properties. *Biomacromolecules*, 13(12), 3990-4001. doi:10.1021/bm301278f
- Yan, D., Teng, Z., Sun, S., Jiang, S., Dong, H., Gao, Y., . . . Guo, H. (2017). Foot-and-mouth disease virus-like particles as integrin-based drug delivery system achieve targeting anti-tumor efficacy. *Nano medicine: Nanotechnology, Biology, and Medicine*, 13(3), 1061-1070. doi:10.1016/j.nano.2016.12.007
- Yildiz, I., Lee, K. L., Chen, K., Shukla, S., & Steinmetz, N. F. (2013). Infusion of imaging and therapeutic molecules into the plant virus-based carrier cowpea mosaic virus: cargo-loading and delivery. *Journal of Controlled Release*, 172(2), 568-578. doi:10.1016/j.jconrel.2013.04.023
- Yoganandhan, K., Leartvibhas, M., Sriwongpuk, S., & Limsuwan, C. (2006). White tail disease of the giant freshwater prawn *Macrobrachium rosenbergii* in Thailand. *Disease of Aquatic Organisms*, 69(2-3), 255-258. doi:10.3354/dao069255
- Yong, C. Y., Yeap, S. K., Goh, Z. H., Ho, K. L., Omar, A. R., & Tan, W. S. (2015). Induction of humoral and cell-mediated immune responses by hepatitis B virus epitope displayed on the virus-like particles of prawn nodavirus. *Applied and Environmental Microbiology*, 81(3), 882-889. doi:10.1128/aem.03695-14
- Yong, C. Y., Yeap, S. K., Ho, K. L., Omar, A. R., & Tan, W. S. (2015). Potential recombinant vaccine against influenza A virus based on M2e displayed on nodaviral capsid nanoparticles. *International Journal of Nanomedicine*, 10, 2751-2763. doi:10.2147/ijn.s77405
- Zeng, Q., Wen, H., Wen, Q., Chen, X., Wang, Y., Xuan, W., . . . Wan, S. (2013). Cucumber mosaic virus as drug delivery vehicle for doxorubicin. *Biomaterials*, 34(19), 4632-4642.
- Zhang, Q., Liu, Q., Liu, S., Yang, H., Liu, S., Zhu, L., . . . Huang, J. (2014). A new nodavirus is associated with covert mortality disease of shrimp. *Journal of General Virology*, 95(Pt 12), 2700-2709. doi:10.1099/vir.0.070078-0
- Zhao, Q., Chen, W., Chen, Y., Zhang, L., Zhang, J., & Zhang, Z. (2011). Self-assembled virus-like particles from rotavirus structural protein VP6 for targeted drug delivery. *Bioconjugate Chemistry*, 22(3), 346-352. doi:10.1021/bc1002532